

CALCULATION OF REACTOR PRESSURE VESSEL FLOWS USING PHOENICS 3.1

A C Thompson
C M Hodge

DNST, HMS SULTAN, Hampshire PO12 3BY, UK

INTRODUCTION

The DNST MSc course of 1998/99 (NAC40), has undertaken a design study based on a hypothetical two core pressurised water reactor. The general layout of the plant was established by the previous year's course (NAC39) which utilised Reactor Pressure Vessels (RPVs) with several inlet and outlet nozzles. Initial work for NAC41 involved the development of a Computational Fluid Dynamics (CFD) model of a PWR. The objective of the CFD modelling was to establish the flow patterns within the RPV of a PWR. This was required so that any changes in flow could be assessed when the number of inlet and outlet nozzles was reduced to only one of each. If the flow within the RPV remained satisfactory after such an alteration it would allow the removal of the manifolds between the primary loop and the inlets and outlets of the RPV which are present in the NAC39 design. This simplification would remove the associated shock and frictional losses from the primary circuit reducing head loss and thus improving flow. This alteration would also simplify the manufacture of such a RPV due to the reduction in transition pieces required. The reduction in the number of welds required would also lower through life costs and the dose burden due to the reduced requirement for In Service Inspection.

The flow between the inlet to the RPV and the core inlet has attracted a number of investigators recently. Kil-Sup Um et al. [1] showed by computation and scale model tests that asymmetry in the inlet flow has a marked effect on the conditions at the core inlet. Gavelli and Kiger [2] made detailed measurement of the concentration of boron in a model downcomer and revealed some interesting complications in the flow pattern there. It has been known for longer, see Radcliff et al. [3] that vortices in the lower head can cause mal-distribution of the flow at the core inlet. Thus the present work aims to examine the effect of a single inlet on both the uniformity of core inlet flow and the flow in the downcomer. These two regions are thought to be the most likely to be affected by changes to the inlet nozzle, the importance of well distributed flow to the core inlet is obvious, the downcomer contains thermal shields which also require an even flow to promote cooling.

THE RPV FLOW MODEL

Since the inlet flow patterns under steady state conditions are the main object of study, steady, incompressible flow with no heat transfer is assumed. The fluid selected from the standard properties library was water at 27 °C. Water at ambient temperature might well be used in a scale model test to examine the same phenomena. Cylindrical polar coordinates were adopted with 90x50x50 cells in the X (azimuthal), Y (radial) and Z (axial) directions of the fluid domain. A core barrel diameter of 1.0 m was assumed in advance of the final design details being fixed. This core diameter allowed for a square core of 25 modules of the type used in the Shippingport Pressurised Water Reactor described in [4], which is the basis of the NAC41 module design.

The RPV model was constructed in VR Editor using the objects listed in Table 1. These are then related to the grid automatically by the software. The base of the RPV was created using the 'Corebase' and 13 'Diffuser' blocks to model the bowl shape of the lower head where the flow is turned round from the vertically downwards to vertically upwards at inlet to the core. Each object has a starting position and a size in the X,Y and Z directions. The geometry "polcube" of this first

group of objects specifies a simple box in polar coordinates, the type “blockage” means the box is filled by material given by “attributes”. In this case material 198, a solid with smooth wall friction (SwSWF) and no heat transfer is entered.

The next object in Table 1 is the core barrel, a sleeve running from the top of the RPV model to just above the base. Flow enters the annulus between the core barrel and the RPV wall (called the downcomer) and passes downwards to the lower head before flowing up into the core. Two further objects, the thermal shields, sit in the lower half of the downcomer and divide it into three annular passages. The RPV wall and the RPV head complete the outer part of the model.

Outlets are represented by special objects positioned on the inner wall of the core barrel, near the top of the RPV. They have zero radial (Y) size, cylindrical geometry and “outlet” type. Pressure is fixed at 0.0 Pa through the attributes part of the object menu. Inlets are represented by similar cylinders on the inner wall of the RPV. They have a constant mass flowrate of 250 kg/s specified under attributes. For computational purposes, the outlets do not need to communicate to the outside of the RPV, however, outlet nozzles are included since they are blockages to flow in the inlet plenum. Figure 1 shows the objects described so far, without the RPV wall.

The remainder of the model is defined by objects representing the flow path between the core inlet and the outlets. Flow enters the core through a set of holes in the inlet ring object, a disc blanking the bottom of the core barrel. The remainder of the flow path serves simply to provide a resistance and is not studied in detail. Flow proceeds upwards through the core to the outlet. Figure 2 shows these objects with thermal shields and core barrel removed.

The sixteen core inlet holes are modelled by cylindrical objects B30 to B45, passing through the inlet ring object. These are defined as type “blockage” with material attributes “water at 27 °C”.

The flow above the core inlet holes is not of primary interest in this study and core region is required simply to provide an appropriate back-pressure for the flow rate imposed. Regions A and B are represented as a porous solid by introducing quadratic sources in the axial momentum equation, (Z direction) for the core. Once all the objects defining the geometry of the flow boundaries are entered, the software automatically sets the grid to the edge of any object within the domain. For areas where high resolution is required the grid can be manually refined from the ‘Geometry’ menu. To achieve the best results the grid was refined to the maximum capacity allowed by the standard installation of the software, which limited the cell numbers to 90x50x50.

RESULTS

Multi - inlet flow patterns. Figure 3 shows the velocity vectors in the flow near one of the inlets on an X plane slice. There are small re-circulation regions above and below the nozzle but no reversed flow in the thermal shields. The velocity in the inner thermal shield passage is however, much higher than that in the outer passages in this region. Flow in the central part of the figure is in the outlet plenum, which is separated from the inlet flow by the core barrel. Figure 4 shows the lower part of the flow on a different X plane. The flow is downward in all the shield passages turning round in the lower head and entering the core inlets. Upward flow can be seen in core sections A and B. The velocity vectors at points in an X plane bisecting an outlet appear in Figure 5. In the central part of the outlet plenum the flow is initially upwards from the exit of core region B, turning towards the horizontal outlet at the top. At larger radius in the outlet plenum there is slower recirculating flow. Beneath the outlet nozzle flow is downward. This is outside the core barrel and gives another view of flow in the thermal shield passages.

Figure 6 shows flow in a horizontal (Z) plane through the inlets and outlets, indicating the strong vortex patterns at the top of the downcomer. This view also gives an impression of the grid spacing in the model.

Single inlet flow patterns. Results for the single inlet and outlet are given in figures 7 to 12. The flow in an X plane through the inlet appears in figure 7 where the strong upward flow in the middle and outer shield passages is immediately evident. This contrasts with the slow downward flow under an inlet in the dual inlet case of figure 3. Reversed flow in the shield passages may have undesirable effects on the cooling of the shields and corrective measures are required, as described below.

Figure 8 shows velocities in the core inlets. The flow appears to be evenly distributed between the inlets. Only one hole (near $X = 0$) has velocities which appear different in angle if not magnitude from the rest. The flow distribution was judged adequate at this stage in the study and attention was concentrated on correcting the shield flow.

Flow distribution devices. The first attempt at a fix consisted of fitting a ‘bell-mouth’ underneath the inlet to fill the re-circulation region and induce a smoother flow into the thermal shields. This device has insufficient effect, still leaving an upward flow in the two outer shield passages, see Figure 9. There does not appear to be space for an effective device of this type so a guiding blade referred to as the scoop was tried.

This second fix is a curved plate extending round half the circumference and shaped as a scoop in an X plane section. It is horizontal at the mid-level of the inlet so that it catches inflow below this level and directs it downwards into the outer shield passage. Figure 10 shows the arrangement and the velocities produced. Downward flow is produced in the outer thermal shield but there is little effect on flow in the middle thermal shield. The distribution of flow into the core remains uniform as can be seen in Figure 11.

The third attempt at a solution involved the placing of a second scoop above and behind the first scoop. Repeated adjustment of height and radial position of the scoops obtained a solution with flow in all thermal shields successfully directed downwards. This was achieved with the objects defined as “final fix” in Table 1 and displayed in Figure 12. Figure 13 demonstrates that the flow descends in all shield passages. Velocity is considerably greater in the inner passage than the outer two.

The flow distribution at the core inlet is shown in Figure 14. The maximum velocity in each core inlet appears quite similar except for the inlet near $X = 0$ where the flow is angled inwards. This was further investigated by taking velocity readings with the flow probe in each core inlet. The vertical coordinate of the probe was fixed to coincide with the mid-plane of the inlet ring, $Z = 0.261$ m. The radial coordinate was set at the estimated maximum velocity position for the first hole, $Y = 0.318$ m and the angular coordinate X was then adjusted to the centre of each hole where a velocity reading was taken. This was repeated at a radius $Y = 0.33$ m where the maximum velocity in the majority of holes was found. The results are plotted in figure 15. The velocities at a given radius are within 3% of the average value except for the first, sixth and fourteenth holes. This can be explained if the computational grid is examined in the mid-plane of the inlet ring, as shown in Figure 16. The first core inlet, which appears at the top right of the figure next to the help button, is represented by four rows of cells. Each of the remaining inlets span only two cells in the X direction, except for numbers six (at the bottom left) and fourteen. These have an extra very narrow cell on one side. The extra cells in the first inlet allow radial momentum from immediately below the inlet ring where there is an inward velocity to affect the calculation of velocities inside the inlet hole. This explains the inward slanting velocity vectors found only in this hole. The high velocity region is larger in this inlet than the remainder, again due to the greater number of cells.

CONCLUSIONS

The VR interface of PHOENICS 3.1 has allowed a CFD model of a complicated internal flow to be set up rapidly and results obtained within the short time scale of an MSc design exercise.

The VR viewer enabled a problem in the proposed design to be identified. The initial single RPV inlet design produced reversed flow in parts of the thermal shield passages which was potentially detrimental to heat transfer.

Flow distribution devices were able to overcome the tendency for re-circulation to occur immediately below the RPV inlet. They acted as guide vanes to assist the flow to turn sharply and enter the outer shield passages. Some iteration of the number and spacing of scoops was required to achieve this. A solution employing two scoops with their outlet edges directly above the two shields was adopted.

The calculation of the core inlet flows was influenced by the number of grid cells allocated to each inlet. It is believed that this effect causes the three anomalous flows in the sixteen core inlets and the single RPV inlet has no adverse effect on the distribution of flow into the core.

REFERENCES

1. Filippo Gavelli and Kenneth Kiger, "High-resolution boron dilution measurements using laser induced fluorescence (LIF)". Nuclear Engineering and Design Vol. 195 no1 Jan 2000 p3-26.
2. Kil-Sup Um, Seok-Hee Ryu, Yong-Seog Choi and Goon-Cherl Park, "Experimental and computational study of core inlet temperatures under asymmetric loop conditions". Nuclear Technology Vol. 125 Mar 1999 p305-315.
3. T D Radcliff, W S Johnson, J R Parsons and D E Ekeroth, "Visualisation of the lower plenum anomaly in the Westinghouse AP600 reactor". Nuclear Technology April 1994 Vol.106 p100-109.
4. R T Bayard et al. "The Shippingport Pressurised Water Reactor". Addison Wesley 1958.
5. PHOENICS TR324 "Starting with PHEONICS VR". CHAM, Dec 1997.

COPYRIGHT

BRITISH Crown Copyright 2000/MOD

Published with the permission of the Controller of Her Britannic Majesty's Stationery Office

RPV CONSTRUCTION AND MODEL

Table 1 – RPV CFD Model Components

Component	X Position	X Size	Y Position	Y Size	Z Position	Z Size	Geometry	Type	Attributes
Corebase	0	6.284	0	0.3	0	0.25	polcube	blockage	198SwSWF
Diffuser1	0	6.284	0.3	0.01	0	0.23	polcube	blockage	198SwSWF
Diffuser2	0	6.284	0.31	0.02	0	0.18	polcube	blockage	198SwSWF
Diffuser3	0	6.284	0.33	0.02	0	0.15	polcube	blockage	198SwSWF
Diffuser4	0	6.284	0.35	0.03	0	0.1	polcube	blockage	198SwSWF
Diffuser5	0	6.284	0.38	0.03	0	0.08	polcube	blockage	198SwSWF
Diffuser6	0	6.284	0.41	0.05	0	0.05	polcube	blockage	198SwSWF
Diffuser7	0	6.284	0.46	0.1	0	0.04	polcube	blockage	198SwSWF
Diffuser8	0	6.284	0.56	0.05	0	0.05	polcube	blockage	198SwSWF
Diffuser9	0	6.284	0.61	0.03	0	0.08	polcube	blockage	198SwSWF
Diffuser10	0	6.284	0.64	0.03	0	0.1	polcube	blockage	198SwSWF
Diffuser11	0	6.284	0.67	0.02	0	0.15	polcube	blockage	198SwSWF
Diffuser12	0	6.284	0.69	0.02	0	0.18	polcube	blockage	198SwSWF
Diffuser13	0	6.284	0.71	0.01	0	0.23	polcube	blockage	198SwSWF
Core Barrel	0	6.284	0.5	0.02	0.25	2.8	polcube	blockage	198SwSWF
Inner Shield	0	6.284	0.56	0.04	0.3	1.85	polcube	blockage	198SwSWF
Outer Shield	0	6.284	0.64	0.04	0.25	1.9	polcube	blockage	198SwSWF
RPV	0	6.284	0.72	0.18	0	3.05	polcube	blockage	198SwSWF
RPV Head	0	6.284	0	0.9	3.05	0.1	polcube	blockage	198SwSWF
Outlet1	3.14	0.471	0.5	0	2.45	0.3	Cyl1	outlet	0 pressure
Outlet2	4.71	0.471	0.5	0	2.45	0.3	Cyl1	outlet	0 pressure
Inlet1	1.57	0.471	0.72	0	2.45	0.3	Cyl1	inlet	0.25m3/s
Inlet2	0	0.471	0.72	0	2.45	0.3	Cyl1	inlet	0.25m3/s
Outlet nozzle	3.14	0.471	0.52	0.2	2.45	0.3	Cyl1	blockage	198SwSWF
Outlet nozzle	4.71	0.471	0.52	0.2	2.45	0.3	Cyl1	blockage	198SwSWF
Inlet ring	0	6.284	0	0.5	0.25	0.02	polcube	blockage	198SwSWF
Core region A	0	6.284	0.26	0.15	0.35	1	polcube	user defined	Phasem
Region A Outer wall	0	6.284	0.41	0.02	0.34	1.05	polcube	blockage	198SwSWF
Core region B	0	6.284	0	0.24	0.35	1	polcube	user defined	Phasem
Region B outer wall	0	6.284	0.24	0.02	0.34	1.26	polcube	blockage	198SwSWF
Region A top	0	6.284	0.26	0.24	1.58	0.02	polcube	blockage	198SwSWF
B30	0	0.285	0.3	0.1	0.24	0.1	Cyl1	blockage	Water
B31	0.393	0.285	0.3	0.1	0.24	0.1	Cyl1	blockage	Water
B32	0.786	0.285	0.3	0.1	0.24	0.1	Cyl1	blockage	Water
B33	1.179	0.285	0.3	0.1	0.24	0.1	Cyl1	blockage	Water
B34	1.572	0.285	0.3	0.1	0.24	0.1	Cyl1	blockage	Water
B35	1.965	0.285	0.3	0.1	0.24	0.1	Cyl1	blockage	Water

Component	X Position	X Size	Y Position	Y Size	Z Position	Z Size	Geometry	Type	Attributes
B36	2.358	0.285	0.3	0.1	0.24	0.1	Cyl1	blockage	Water
B37	2.751	0.285	0.3	0.1	0.24	0.1	Cyl1	blockage	Water
B38	3.144	0.285	0.3	0.1	0.24	0.1	Cyl1	blockage	Water
B39	3.537	0.285	0.3	0.1	0.24	0.1	Cyl1	blockage	Water
B40	3.93	0.285	0.3	0.1	0.24	0.1	Cyl1	blockage	Water
B41	4.23	0.285	0.3	0.1	0.24	0.1	Cyl1	blockage	Water
B42	4.716	0.285	0.3	0.1	0.24	0.1	Cyl1	blockage	Water
B43	5.109	0.285	0.3	0.1	0.24	0.1	Cyl1	blockage	Water
B44	5.502	0.285	0.3	0.1	0.24	0.1	Cyl1	blockage	Water
B45	5.895	0.285	0.3	0.1	0.24	0.1	Cyl1	blockage	Water
Fixes	2nd Attempt								
Fix1	0	3.14	0.65	0.02	2.5	0.01	polcube	blockage	198SwSWF
Fix2	0	3.14	0.64	0.01	2.4	0.11	polcube	blockage	198SwSWF
Fix3	0	3.14	0.65	0.01	2.3	0.11	polcube	blockage	198SwSWF
Fix4	0	3.14	0.66	0.01	2.2	0.11	polcube	blockage	198SwSWF
	3rd Attempt								
Fix1	0	3.14	0.65	0.02	2.5	0.01	polcube	blockage	198SwSWF
Fix2	0	3.14	0.64	0.01	2.4	0.11	polcube	blockage	198SwSWF
Fix3	0	3.14	0.65	0.01	2.3	0.11	polcube	blockage	198SwSWF
Fix4	0	3.14	0.66	0.01	2.2	0.11	polcube	blockage	198SwSWF
Innerfix1	0	3.14	0.6	0.02	2.52	0.01	polcube	blockage	198SwSWF
Innerfix2	0	3.14	0.59	0.01	2.4	0.13	polcube	blockage	198SwSWF
Innerfix3	0	3.14	0.6	0.01	2.3	0.11	polcube	blockage	198SwSWF
Innerfix4	0	3.14	0.61	0.01	2.2	0.11	polcube	blockage	198SwSWF
	Final fix								
Fix1	0	3.14	0.65	0.02	2.5	0.01	polcube	blockage	198SwSWF
Fix2	0	3.14	0.64	0.01	2.4	0.11	polcube	blockage	198SwSWF
Fix3	0	3.14	0.65	0.01	2.3	0.11	polcube	blockage	198SwSWF
Fix4	0	3.14	0.66	0.01	2.17	0.14	polcube	blockage	198SwSWF
Innerfix1	0	3.14	0.57	0.02	2.52	0.01	polcube	blockage	198SwSWF
Innerfix2	0	3.14	0.56	0.01	2.4	0.13	polcube	blockage	198SwSWF
Innerfix3	0	3.14	0.57	0.01	2.3	0.11	polcube	blockage	198SwSWF
Innerfix4	0	3.14	0.58	0.01	2.17	0.14	polcube	blockage	198SwSWF

Table 1 – RPV CFD Model Components (end)

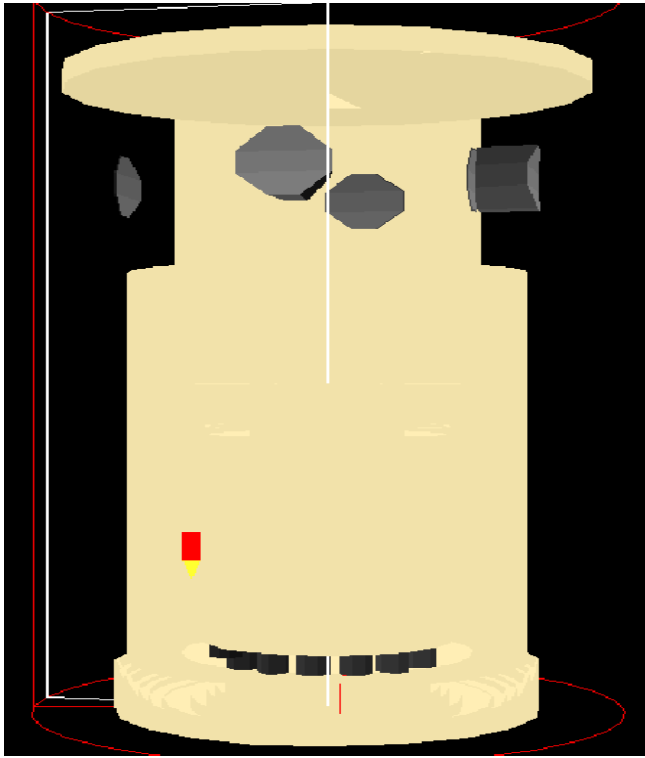


Figure 1. RPV Model with RPV Wall Hidden

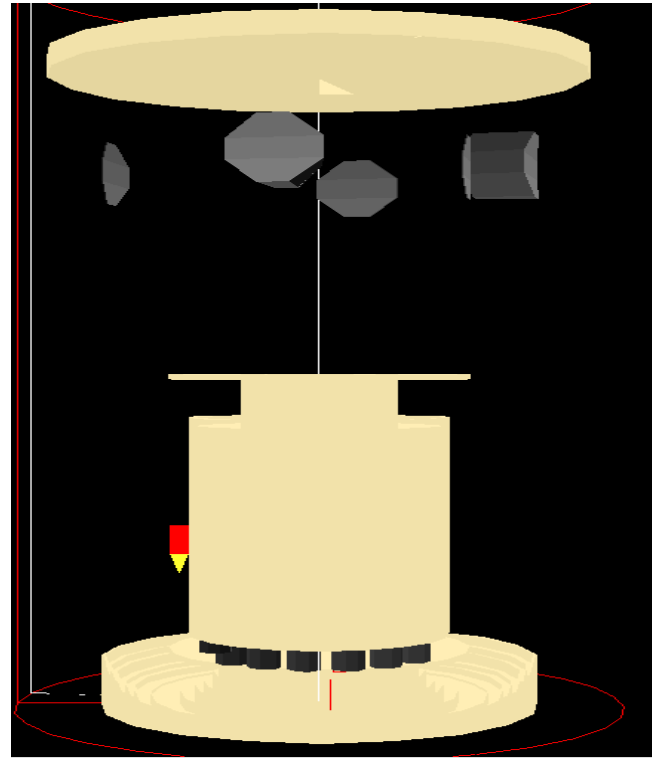


Figure 2 RPV Model with RPV Wall, Thermal Shields and Core Barrel Sides Hidden

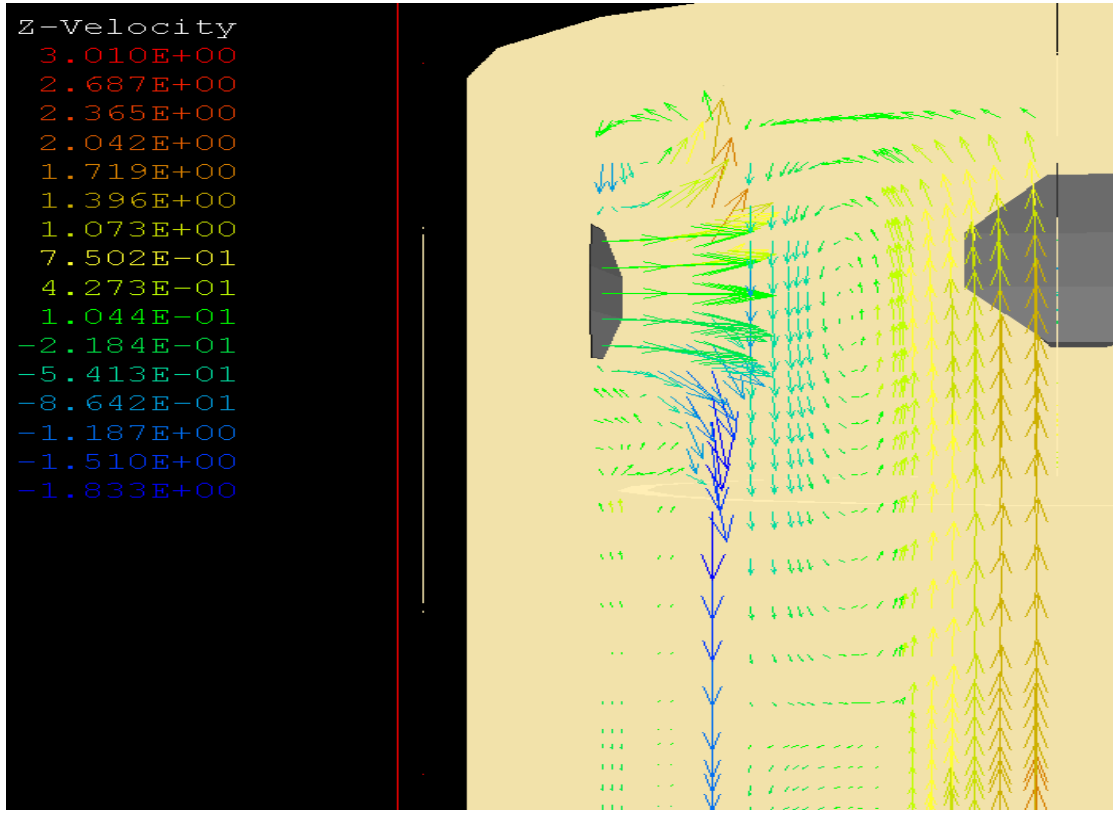


Figure 3. Multi -Inlet RPV - Inlet Flow

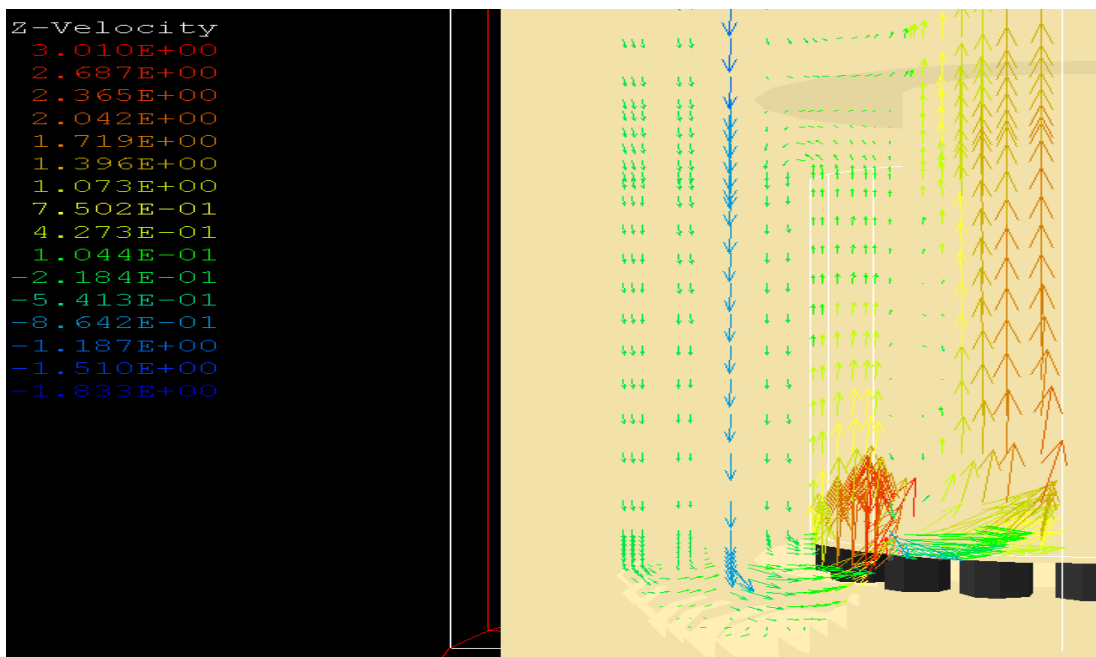


Figure 4 Multi - Inlet RPV - Core Flow

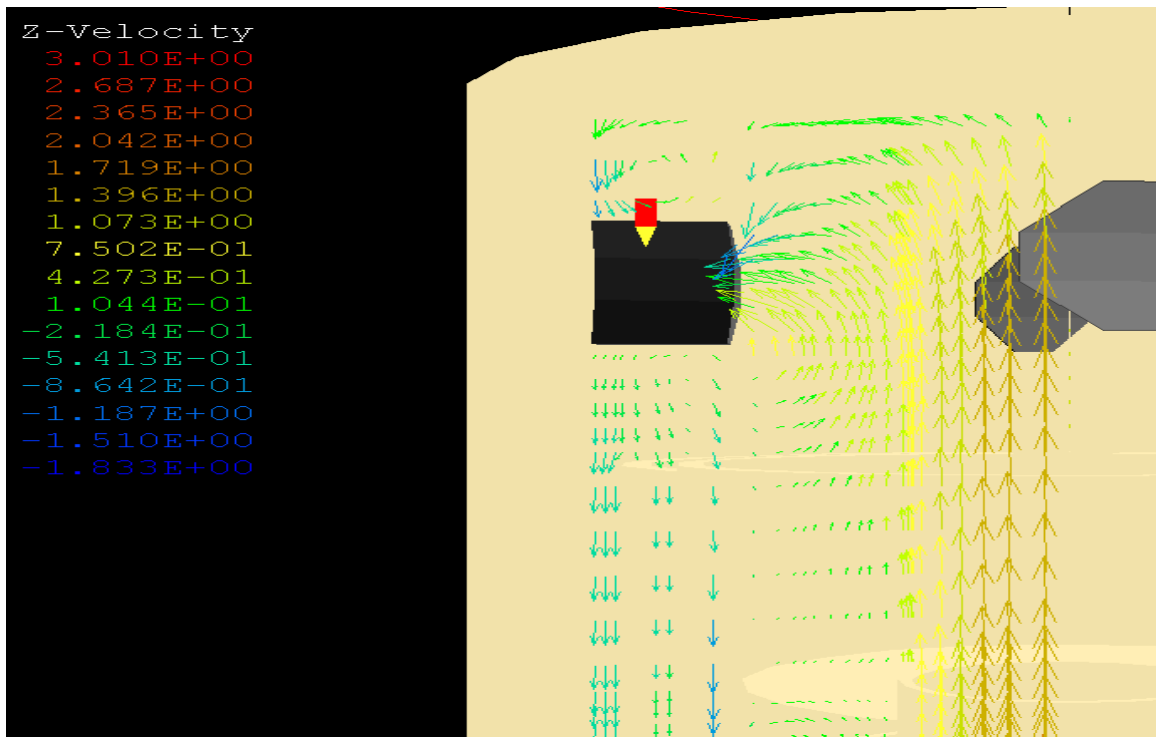


Figure 5 Multi - Inlet RPV - Outlet Flow

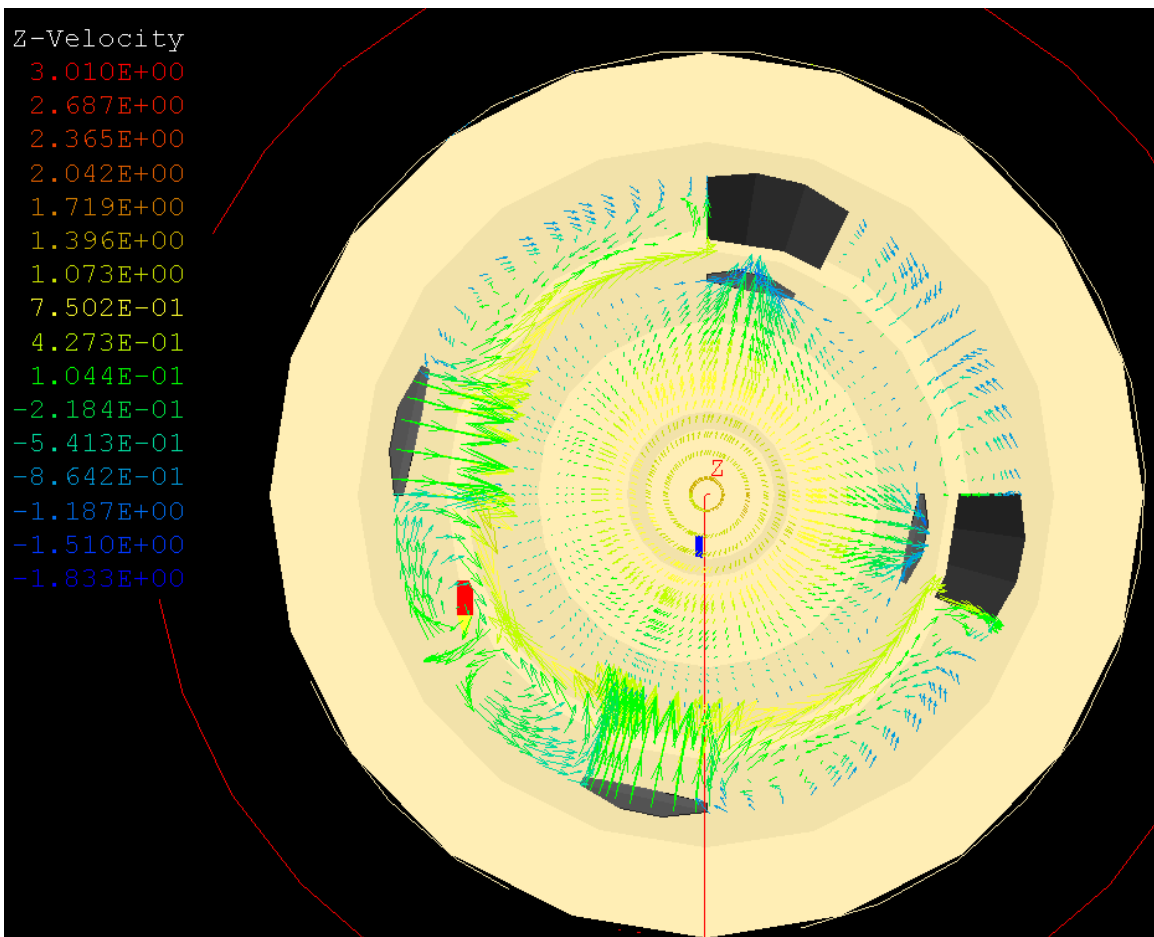


Figure 6. Multi - Inlet RPV- Inlet / Outlet Plenum Flow

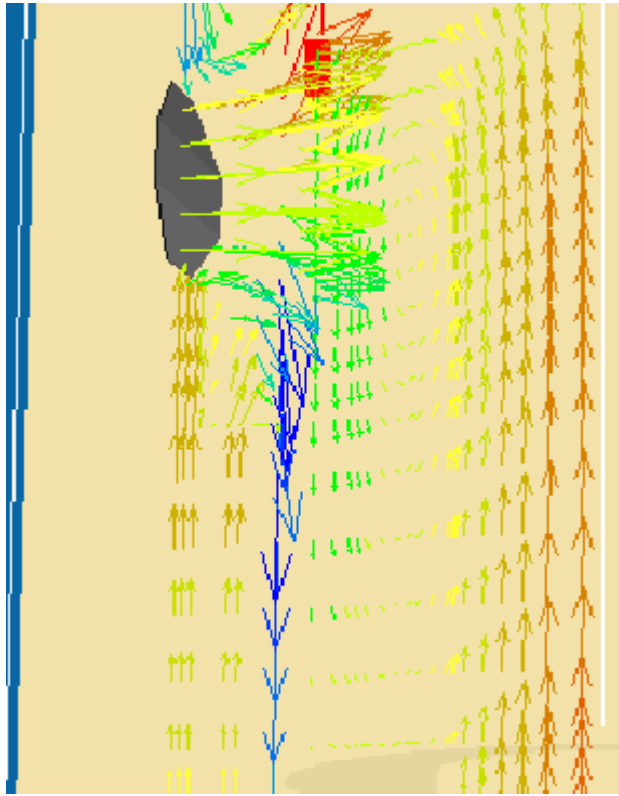


Figure 7. Single Inlet RPV – Inlet Flow

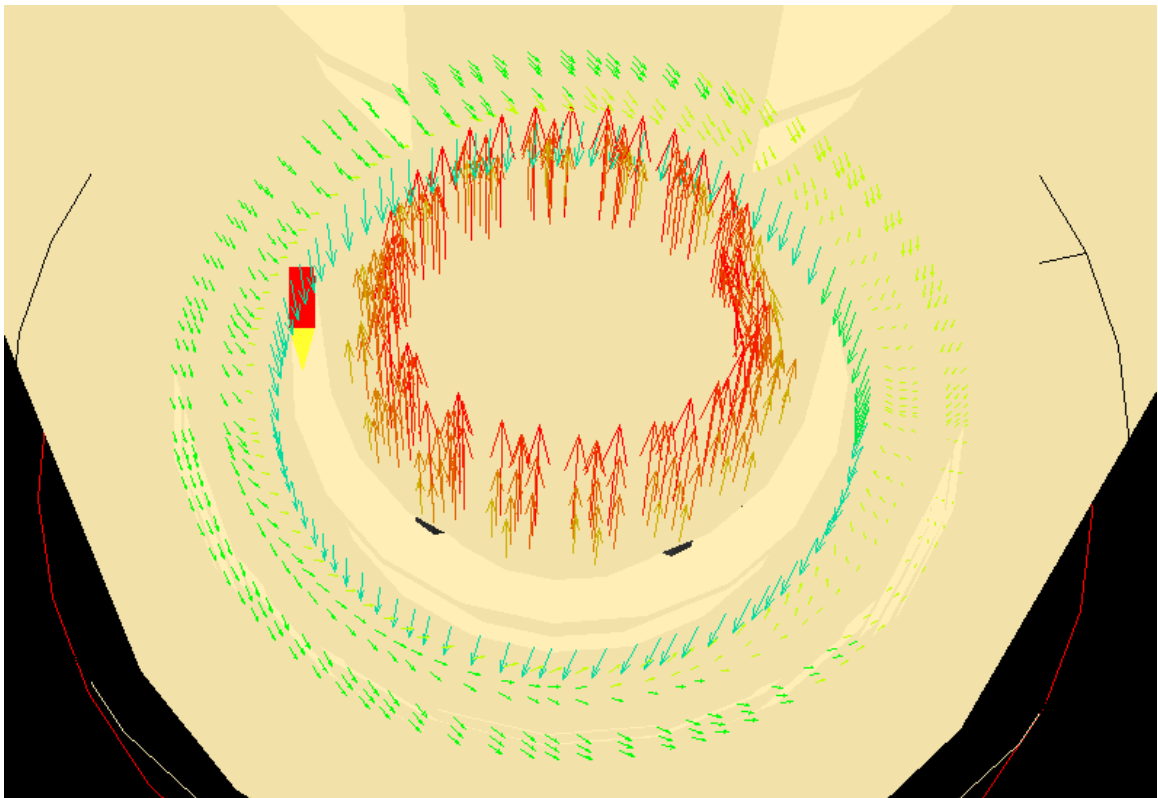


Figure 8 Single Inlet RPV – Core Inlet Flow

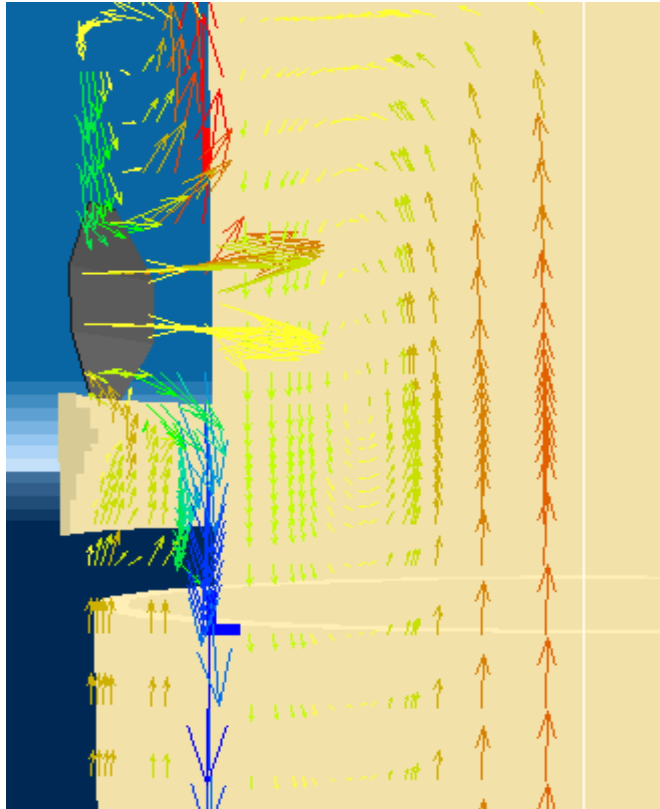


Figure 9 Single Inlet RPV – Bell Mouth Inlet Flow

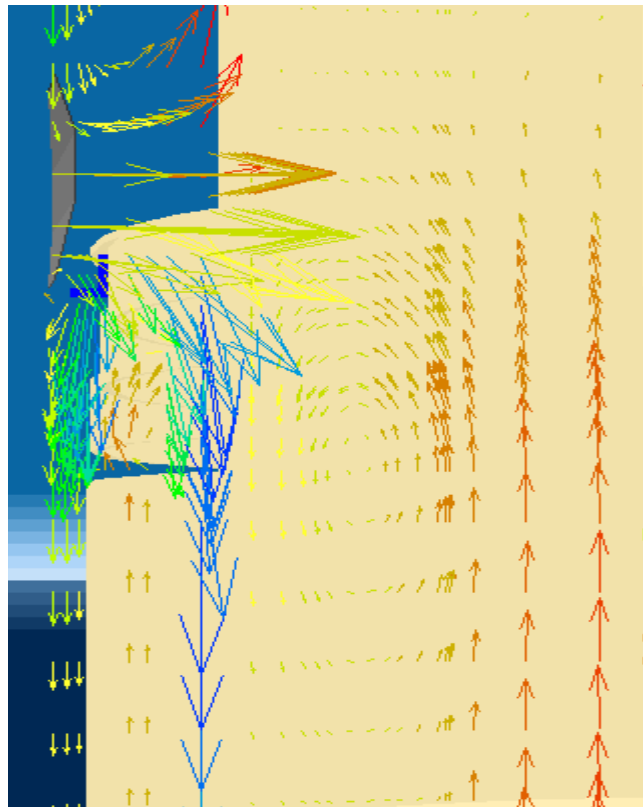


Figure 10 Single Inlet RPV- Scoop Inlet Flow

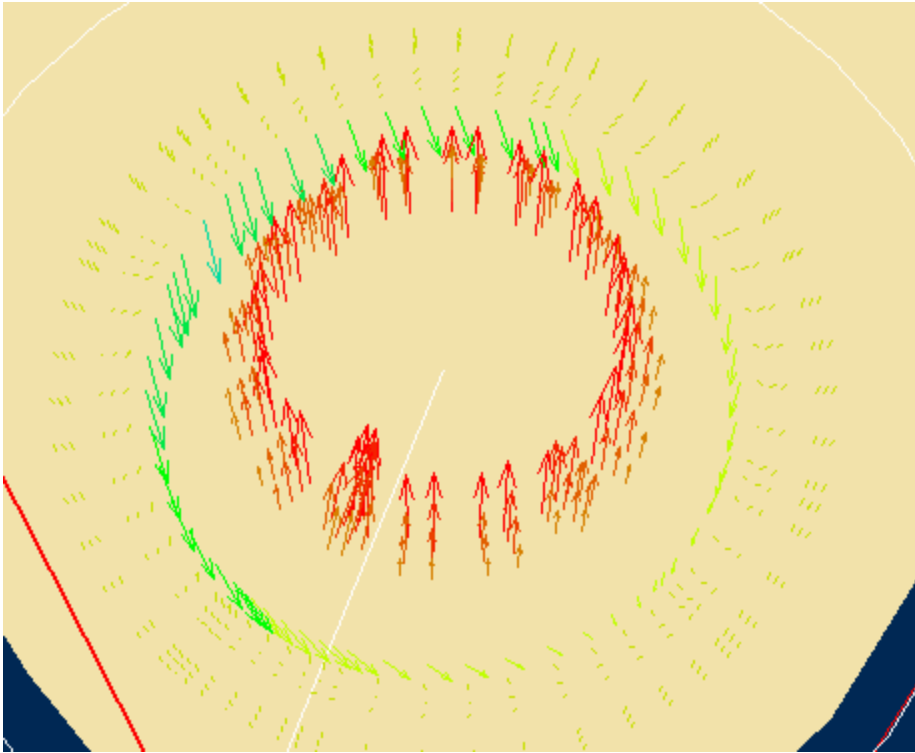


Figure 11 Single Inlet RPV with Scoop - Core Inlet Flow

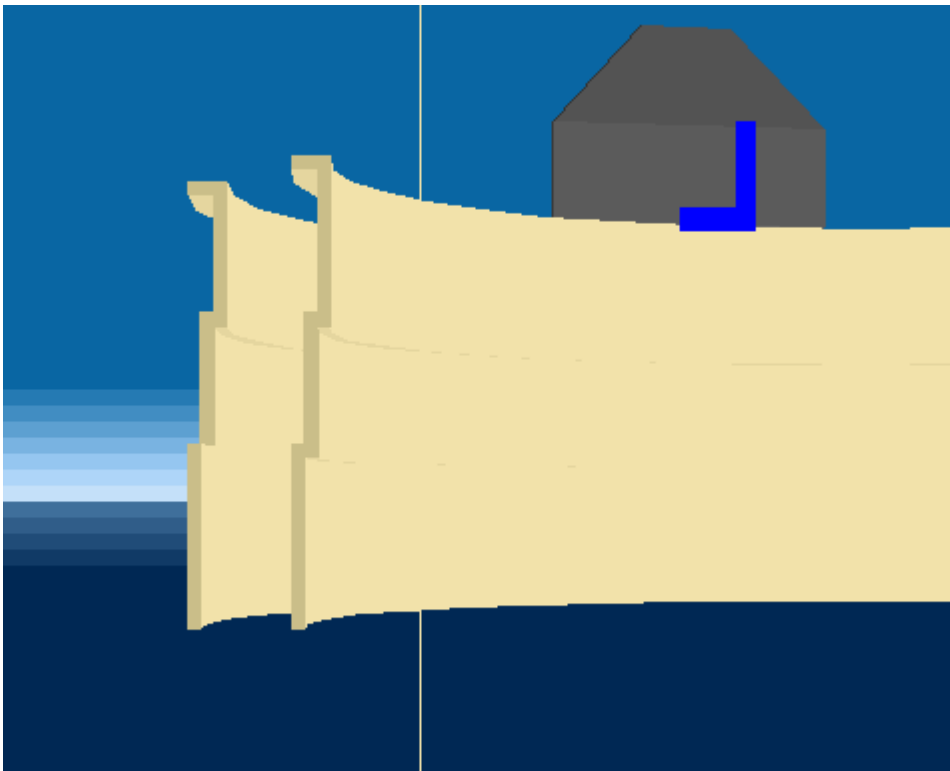


Figure 12 CFD Model of Final Fix

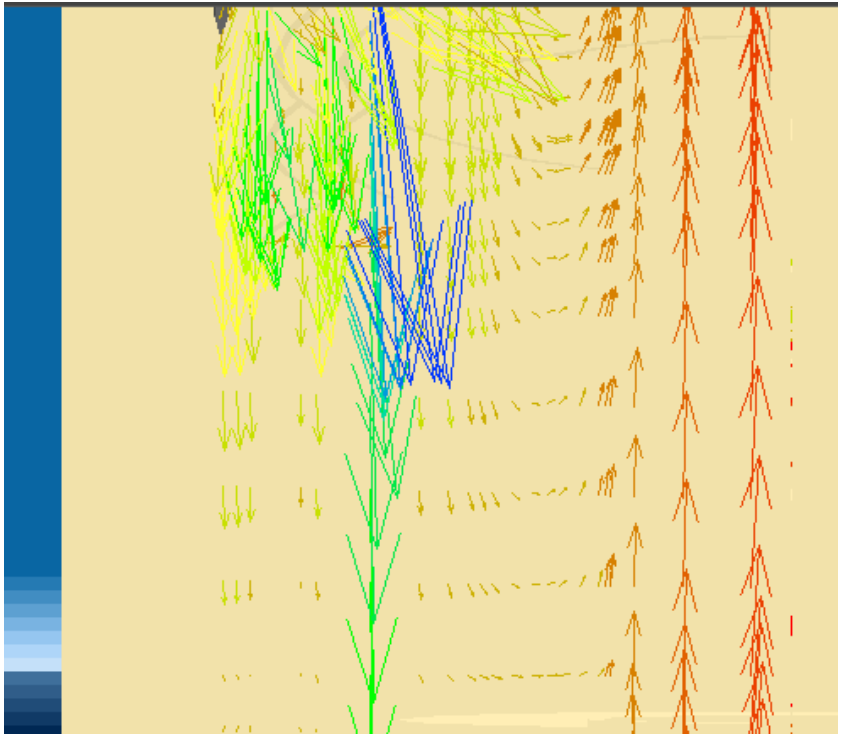


Figure 13 Final Fix - Flow from Inlet descending in all Thermal Shields

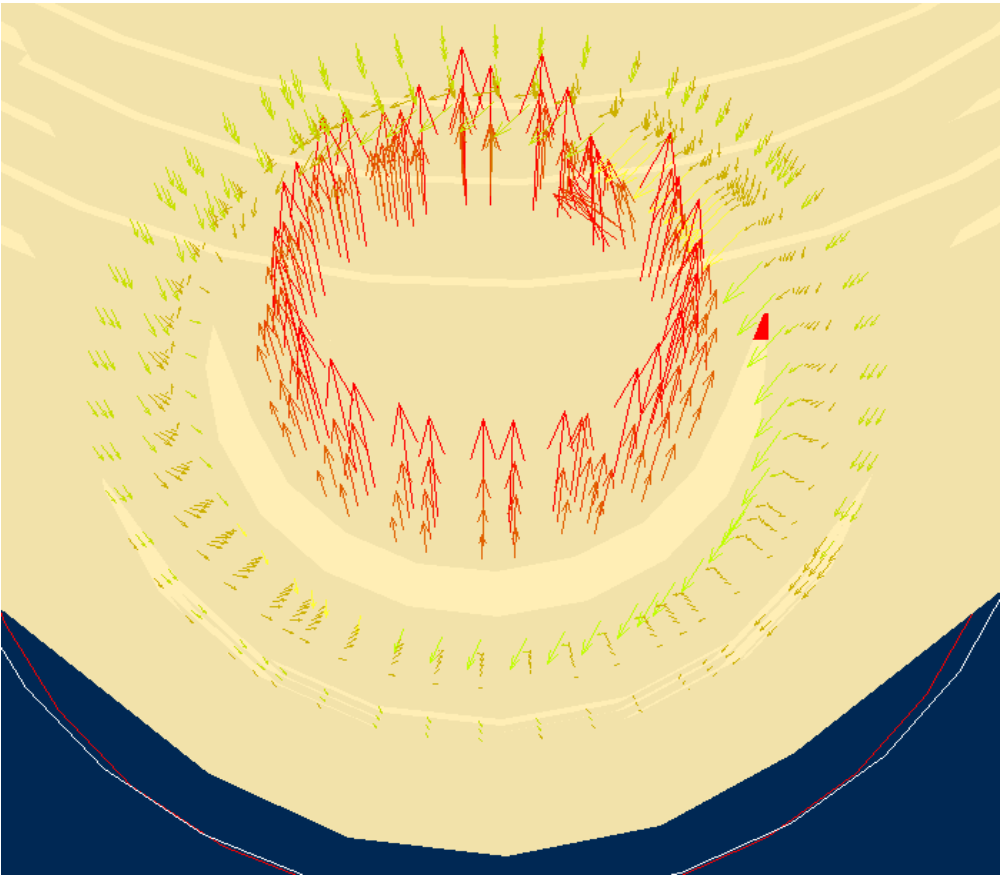


Figure 14 Final Fix Flow Distribution into Core

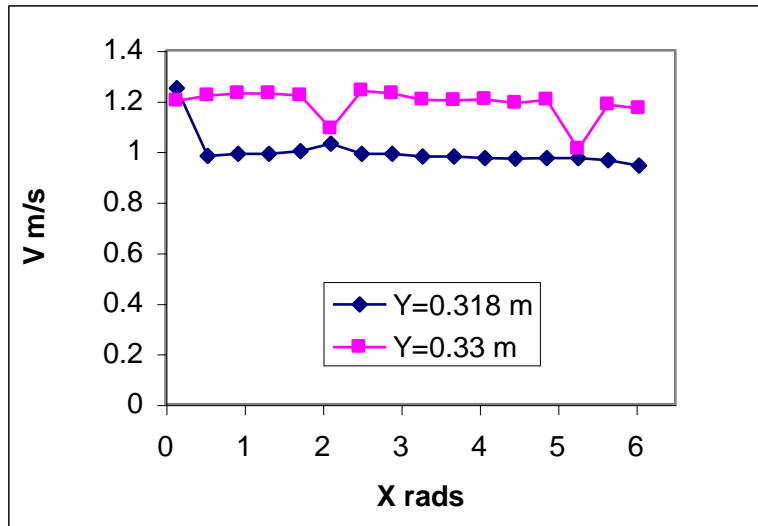


Figure 15 Velocities In Core Inlets

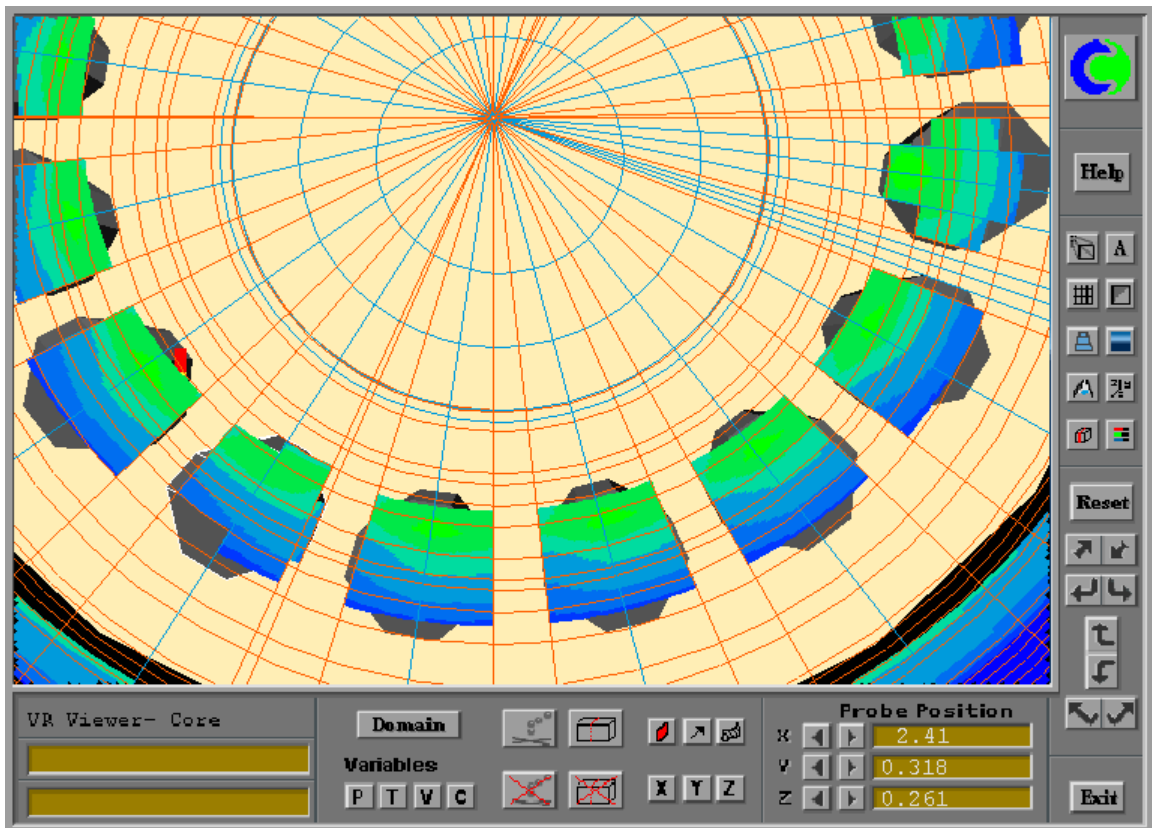


Figure 16 Grid And Velocity Contours in Plane of Core Inlets